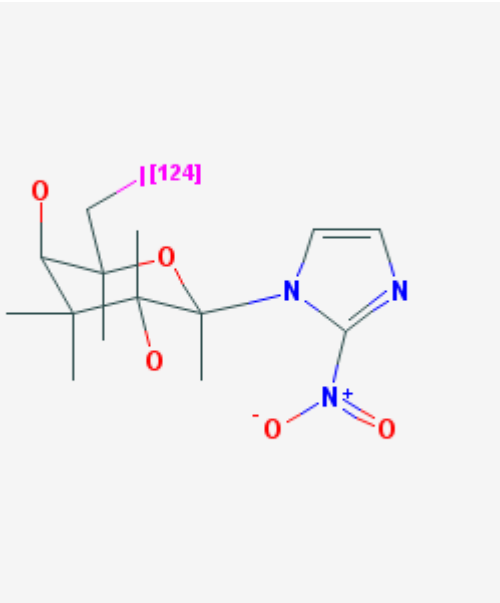


[¹²⁴I]Iodo-azomycin-galactoside

[¹²⁴I]IAZG

Kam Leung, PhD¹

Created: November 22, 2007; Updated: January 30, 2008.

Chemical name:	[¹²⁴ I]Iodo-azomycin-galactoside	
Abbreviated name:	[¹²⁴ I]IAZG	
Synonym:	[¹²⁴ I]-1-(4-Deoxy-4-iodo-β-D-xylopyranosyl)-2-nitroimidazole	
Agent Category:	Compound	
Target:	Hypoxic cells	
Target Category:	Intracellular reduction and binding	
Method of detection:	PET	
Source of signal:	¹²⁴ I	
Activation:	No	
Studies:	<ul style="list-style-type: none">• <i>In vitro</i>• Rodents	
		Click on the above structure for additional information in PubChem .

Background

[[PubMed](#)]

¹ National Center for Biotechnology Information, NLM, NIH, Bethesda, MD; Email: micad@ncbi.nlm.nih.gov.

NLM Citation: Leung K. [¹²⁴I]Iodo-azomycin-galactoside . 2007 Nov 22 [Updated 2008 Jan 30]. In: Molecular Imaging and Contrast Agent Database (MICAD) [Internet]. Bethesda (MD): National Center for Biotechnology Information (US); 2004-2013.

In a variety of solid tumors, hypoxia was found to lead to tumor progression and to resistance of tumors to chemotherapy and radiotherapy (1-3). Tumor oxygenation is heterogeneously distributed within human tumors (4). Hypoxia in malignant tumors is thought to be a major factor limiting the efficacy of chemotherapy and radiotherapy. It would be beneficial to assess tumor oxygenation before and after therapy to provide an evaluation of tumor response to treatment and an insight into new therapeutic treatments (5). Tumor oxygenation is measured invasively using computerized polarographic oxygen-sensitive electrodes, which is regarded as the gold standard (6). Functional, non-invasive imaging of intra-tumoral hypoxia has been demonstrated to be a feasible measurement of tumor oxygenation (7). This has led to the search and development of hypoxia-targeted, non-invasive markers of tumor hypoxia.

Chapman proposed the use of 2-nitroimidazole compounds for hypoxia imaging (8). 2-Nitroimidazole compounds are postulated to undergo reduction in hypoxic condition, forming highly reactive oxygen radicals that subsequently bind covalently to macromolecules inside the cells (9). [¹⁸F]Fluoromisonidazole [¹⁸F]FMISO) is the most widely used positron emission tomography (PET) tracer for imaging tumor hypoxia (7). However, [¹⁸F]FMISO has slow clearance kinetics and a high lipophilicity, resulting in substantially high background in PET scans. Novel 2-nitroimidazole compounds, such as [¹⁸F]FETA, [¹⁸F]FETNIM, 4-Br[¹⁸F]FPN, [¹⁸F]EF1, and [¹⁸F]EF5, are currently being investigated as potential markers of tumor hypoxia [PubMed]. [¹²⁴I]Iodo-azomycin-galactoside ([¹²⁴I]IAZG) is a second-generation hypoxic marker of iodinated azomycin nucleosides with greater water solubility than other 2-nitroimidazole compounds, which increases renal excretion (10). [¹²⁴I]IAZG is being evaluated as a PET probe for the detection of tumor hypoxia.

Synthesis

[PubMed]

Schneider et al. (11) reported that [¹²⁵I]IAZG was synthesized by exchange reaction between IAZG and ¹²⁵I-NaI with 60% radiochemical yield. [¹²⁵I]IAZG had a specific activity of 10.2 GBq/mmol (276 mCi/mmol). Zanzonico et al. (12) produced [¹²⁴I]IAZG from IAZG and ¹²⁴I-NaI with a radiochemical purity of >98%.

In Vitro Studies: Testing in Cells and Tissues

[PubMed]

[¹²⁵I]IAZG (10 μM) accumulated in EMT-6 tumor cells at a rate of 13.6 pmol/10⁶ cells per h (10). High oxygen concentration decreased and low oxygen concentration increased the rate of accumulation. No blocking studies were performed.

Animal Studies

Rodents

[PubMed]

Schneider et al. (11) performed biodistribution studies of $[^{125}\text{I}]\text{IAZG}$ in mice bearing EMT-6 tumors. The biodistribution was fast except in the brain, where it was significantly lower, and in the liver and the kidney, where it was significantly higher. The tracer was rapidly cleared from the blood (plasma half-life, 0.46 h) with rapid renal and hepatobiliary clearance within 2–3 h. There was a relative accumulation of the tracer in tumor with time (tumor/muscle and tumor/blood ratios were 23.0 and 9.9, respectively, at 6 h after injection). The maximal tumor uptake was at 0.5 h with $3.27 \pm 0.08\%$ injected dose (ID)/g. The liver ($0.77 \pm 0.22\%$ ID/g) and kidney ($0.79 \pm 0.16\%$ ID/g) exhibited lower accumulation than the tumor ($1.54 \pm 0.19\%$ ID/g) at 2 h. No blocking studies were performed.

Zanzonico et al. (12) performed serial microPET imaging to evaluate $[^{124}\text{I}]\text{IAZG}$ as a hypoxia imaging agent in 17 MCa breast tumors and 6 FSaII fibrosarcomas implanted in mice. For comparison, $[^{18}\text{F}]\text{FMISO}$ was also imaged in the same tumor-bearing animals. Twelve animals were also imaged with $[^{18}\text{F}]\text{fluorodeoxyglucose}$ ($[^{18}\text{F}]\text{FDG}$). Both $[^{124}\text{I}]\text{IAZG}$ and $[^{18}\text{F}]\text{FMISO}$ images showed high tracer uptake in the large tumors (>300 mg, $\text{pO}_2 < 2.5$ mmHg in 67% of tumors). In $[^{18}\text{F}]\text{FMISO}$ images at 1, 3–4, and 6–8 h after injection, there was considerable whole-body background radioactivity. In contrast, $[^{124}\text{I}]\text{IAZG}$ imaging was optimal when performed at 24–48 h with low whole-body background. As a result, the $[^{124}\text{I}]\text{IAZG}$ images at 24–48 h had higher tumor/whole body activity contrast than the $[^{18}\text{F}]\text{FMISO}$ images at 3–6 h. A tumor uptake of 5–10% (of total body radioactivity) was visualized for $[^{18}\text{F}]\text{FMISO}$ at 3–6 h; tumor uptake for $[^{124}\text{I}]\text{IAZG}$ at 48 h was ~17%. Furthermore, biodistribution data showed that the tumor/normal tissue ratios (normal tissue includes the blood, heart, lung, liver, spleen, kidney, intestine, and muscle) of $[^{124}\text{I}]\text{IAZG}$ at 24 h were 1.5–2 times higher than those of $[^{18}\text{F}]\text{FMISO}$ at 3 h, with the exception of the stomach. The small tumors (80–180 mg, $\text{pO}_2 < 2.5$ mmHg in 28% of tumors) were visualized in the $[^{18}\text{F}]\text{FDG}$ images but not in the $[^{124}\text{I}]\text{IAZG}$ or $[^{18}\text{F}]\text{FMISO}$ images. This may be because of the combined effect of a smaller tumor volume and a lower hypoxic fraction. The biodistribution data also showed lower uptake of the tracers in the small tumors than in the large tumors. The tumor accumulation values of $[^{18}\text{F}]\text{FMISO}$ ($7.4 \pm 4.4\%$ ID/g and $11.1 \pm 3.5\%$ ID/g in large and small tumors, respectively) were higher than those of $[^{124}\text{I}]\text{IAZG}$ ($1.5 \pm 0.6\%$ ID/g and $2.3 \pm 0.5\%$ ID/g in large and small tumors, respectively) at 3 h after injection. No blocking studies were performed.

Riedl et al. (13) used dynamic microPET imaging to show that $[^{18}\text{F}]\text{FMISO}$ and $[^{124}\text{I}]\text{IAZG}$ colocalized to the same intra-tumor regions in an orthotopic Morris hepatoma RH-7777 tumor model in mice. The tumor signal increased with time after $[^{18}\text{F}]\text{FMISO}$ injection, whereas the tumor signal slowly decreased after $[^{124}\text{I}]\text{IAZG}$

injection with a faster clearance from the surrounding normal tissues. The tumor/normal tissue ratios of [^{124}I]IAZG increased, but they did so more slowly than those of [^{18}F]FMISO in all 11 tumors in 4 mice and reached similar tumor/normal tissue ratios at a later time point (>6 h) than [^{18}F]FMISO. The tumor/normal tissue ratios at 3 h for [^{18}F]FMISO (1.2–2.3) were higher than those for [^{124}I]IAZG (1.05–1.35). The tumor accumulation of [^{18}F]FMISO ($0.7 \pm 0.2\%$ ID/g) was more than two-fold higher than that of [^{124}I]IAZG ($0.22 \pm 0.05\%$ ID/g) at 3 h after injection. No blocking studies were performed.

Other Non-Primate Mammals

[PubMed]

No publication is currently available.

Non-Human Primates

[PubMed]

No publication is currently available.

Human Studies

[PubMed]

No publication is currently available.

NIH Support

CA06927, CA55893, R01 CA84596, R24 CA83084, R25 CA096945-3, P01 CA115675

References

1. Serkies K., Jassem J. Chemotherapy in the primary treatment of cervical carcinoma. *Crit Rev Oncol Hematol.* 2005;**54**(3):197–208. PubMed PMID: 15890269.
2. Vaupel P., Mayer A. Hypoxia and anemia: effects on tumor biology and treatment resistance. *Transfus Clin Biol.* 2005;**12**(1):5–10. PubMed PMID: 15814285.
3. Rajendran J.G., Krohn K.A. Imaging hypoxia and angiogenesis in tumors. *Radiol Clin North Am.* 2005;**43**(1):169–87. PubMed PMID: 15693655.
4. Vaupel P., Harrison L. Tumor hypoxia: causative factors, compensatory mechanisms, and cellular response. *Oncologist.* 2004;**9**Suppl 54–9. PubMed PMID: 15591417.
5. Dehdashti F., Grigsby P.W., Mintun M.A., Lewis J.S., Siegel B.A., Welch M.J. Assessing tumor hypoxia in cervical cancer by positron emission tomography with ^{60}Cu -ATSM: relationship to therapeutic response—a preliminary report. *Int J Radiat Oncol Biol Phys.* 2003;**55**(5):1233–8. PubMed PMID: 12654432.
6. Raleigh J.A., Dewhirst M.W., Thrall D.E. Measuring Tumor Hypoxia. *Semin Radiat Oncol.* 1996;**6**(1):37–45. PubMed PMID: 10717160.

7. Foo S.S., Abbott D.F., Lawrentschuk N., Scott A.M. Functional imaging of intratumoral hypoxia. *Mol Imaging Biol.* 2004;**6**(5):291–305. PubMed PMID: 15380739.
8. Chapman J.D. Hypoxic sensitizers--implications for radiation therapy. *N Engl J Med.* 1979;**301**(26):1429–32. PubMed PMID: 229413.
9. Chapman J.D., Baer K., Lee J. Characteristics of the metabolism-induced binding of misonidazole to hypoxic mammalian cells. *Cancer Res.* 1983;**43**(4):1523–8. PubMed PMID: 6831401.
10. Chapman J.D., Coia L.R., Stobbe C.C., Engelhardt E.L., Fenning M.C., Schneider R.F. Prediction of tumour hypoxia and radioresistance with nuclear medicine markers. *Br J Cancer Suppl.* 1996;**27**:S204–8. PubMed PMID: 8763881.
11. Schneider R.F., Engelhardt E.L., Stobbe C.C., Fenning M.C., Chapman J.D. The synthesis and radiolabeling of novel markers of tissue hypoxia of the iodinated azomycin nucleoside class. *J. Labelled Compounds and Radiopharmaceuticals.* 1997;**39**(7):541–557.
12. Zanzonico P., O'Donoghue J., Chapman J.D., Schneider R., Cai S., Larson S., Wen B., Chen Y., Finn R., Ruan S., Gerweck L., Humm J., Ling C. Iodine-124-labeled iodoazomycin-galactoside imaging of tumor hypoxia in mice with serial microPET scanning. *Eur J Nucl Med Mol Imaging.* 2004;**31**(1):117–28. PubMed PMID: 14523586.
13. Riedl, C.C., P. Brader, P. Zanzonico, V. Reid, Y. Woo, B. Wen, C.C. Ling, H. Hricak, Y. Fong, and J.L. Humm, Tumor hypoxia imaging in orthotopic liver tumors and peritoneal metastasis: a comparative study featuring dynamic (18)F-MISO and (124)I-IAZG PET in the same study cohort. *Eur J Nucl Med Mol Imaging*, 2007.